SPH Modeling of the Vertical Flow Structure and Turbulence in the Swash

By

Mary Munro

SUBMITTED TO THE DEPARTMENT OF MECHANICAL ENGINEERING IN PARTIAL FULFILLMENT OF THE REQUIREMENTS FOR THE DEGREE OF BACHELORS OF SCIENCE IN MECHANICAL ENGINEERING AND OCEAN ENGINEERING

AT THE

MASSACHUSETTS INSTITUTE OF TECHNOLOGY

FEBRUARY 2015

Signature of Author: Signature redacted

Mary Munro
Department of Mechanical and Ocean Engineering
February 2015

Certified by: Signature redacted

Stefano Brizzolara
Research Scientist
Department of Mechanical Engineering
Massachusetts Institute of Technology
Thesis Supervisor

Accepted by: Signature redacted

Anette Hosoi
Professor of Mechanical Engineering
Undergraduate Officer

SPH Modeling of the Vertical Flow Structure and Turbulence in the Swash

By

Mary Munro

SUBMITTED TO THE DEPARTMENT OF MECHANICAL ENGINEERING ON JUNE 1, 2015 IN PARTIAL FULFILLMENT OF THE REQUIREMENTS FOR THE DEGREE OF BACHELORS OF SCIENCE IN MECHANICAL ENGINEERING AND OCEAN ENGINEERING

ABSTRACT

The vertical structure of swash-zone flows and turbulence, which is critical to sediment transport and flooding due to overtopping of dunes, will be examined using a Smoothed Particle Hydrodynamics model (DualSPHysics) evaluated with field observations obtained near La Jolla, CA in fall 2003. The mesh-free model is based on the Lagrangian description of fluid particle motion, and is capable of tracking free surfaces with discontinuities, moving boundaries, and large deformations, such as those in plunging waves and hydraulic jumps that occur when a swash backwash collides with the following uprush. The model is initialized with a flat sea surface and the measured beach profile and is forced at the offshore boundary with waves observed in 5 m water depth. The model is used to simulate the cross-shore and vertical structure of wave orbital motions, turbulence, and time-mean flows across the surf zone to the swash zone over 10 min periods. Model simulations are compared with field observations of waves and mean flows collected near the bed in 2.5, 1.5, and 1.0 m water depths and at 5 locations in the swash zone. Offshore significant waves heights ranged from 0.5 m to 1.5 m and cross-shore velocities in the surf and swash were up to 0.8 m/s. Model-data comparisons will be presented, the dependence of simulations on free parameters such as smoothing length, distance between particles, and artificial viscosity will be described, and the simulated flows and turbulence will be discussed.

Funding was provided by the Office of Naval Research, The National Science Foundation, MIT Sea Grant, and a WHOI Summer Student Fellowship.

Thesis Supervisor: Stefano Brizzolara

Title: Research Scientist of the Department of Mechanical Engineering

Table of Contents

1. Abstract

The vertical structure of swash-zone flows and turbulence, which is critical to sediment transport and flooding due to overtopping of dunes, will be examined using a Smoothed Particle Hydrodynamics model (DualSPHysics) evaluated with field observations obtained near La Jolla, CA in fall 2003. The mesh-free model is based on the Lagrangian description of fluid particle motion, and is capable of tracking free surfaces with discontinuities, moving boundaries, and large deformations, such as those in plunging waves and hydraulic jumps that occur when a swash backwash collides with the following uprush. The model is initialized with a flat sea surface and the measured beach profile and is forced at the offshore boundary with waves observed in 5 m water depth. The model is used to simulate the cross-shore and vertical structure of wave orbital motions, turbulence, and time-mean flows across the surf zone to the swash zone over 10 min periods. Model simulations are compared with field observations of waves and mean flows collected near the bed in 2.5, 1.5, and 1.0 m water depths and at 5 locations in the swash zone. Offshore significant waves heights ranged from 0.5 m to 1.5 m and cross-shore velocities in the surf and swash were up to 0.8 m/s. Model-data comparisons will be presented, the dependence of simulations on free parameters such as smoothing length, distance between particles, and artificial viscosity will be described, and the simulated flows and turbulence will be discussed.

Funding was provided by the Office of Naval Research, The National Science Foundation, MIT Sea Grant, and a WHOI Summer Student Fellowship.

2. Introduction

One may generally think of swash as the calming waves on a beach, such as those we see in figure 1.

Figure 1: "Tame Swash"

However, for too many people, swash means potential destruction, flooding, and erosion. Of particular interest is the case when swash overtops dunes and so results in flooding, so that during Hurricane Sandy, for example, the likelihood of flooding was under predicted along the NJ shore. One needs to better understand the chances of large swashes to better predict when and where flooding will occur.

Swash also is critical to the erosion at the beach, which depends on the stress on the sand and the turbulence that could suspend sediment. To understand the chance of overtopping and flooding, and to understand the swash-driven sediment movement, one needs to know more about the vertical structure and turbulence in the swash, shown circled in red in figure 2.

Figure 2: Powerful Swash and its vertical structure circled in red

If one can better predict how offshore sea conditions will affect what the waves will look like when they meet the coast, one can make better predictions about flooding, coastal erosion, and sediment transport.

Since the goal is to examine vertical structure, the chosen model is an SPH (Smooth Particle Hydrodynamics) model. It uses the Lagrangian description of fluid motion, implying no need for a mesh, so SPH can handle complex fluid motion naturally. "Smooth" references the fact that the particles are not atoms, but represent a small part of the problem domain. Although the SPH model was initially developed for compressible fluids, it was since then adapted for hydrodynamic problems, and its current development and application is spreading worldwide very rapidly for hydrodynamics of free surface flows. Although SPH is one of the most accurate modeling techniques for fluid flow, there is a catch deterring its use. In the trade-off between time and precision, which one has to make, SPH models take much computational power and are often an impractical use of time when one has to simulate a large flow volume, or flow for a long time.

However, the simulation is of 2D swash on a beach resulting from incident monochromatic waves over an interval of 1 hour. This relatively small space and time domain further justifies the computationally expensive choice of an SPH model to capture the finer details of what's happening. Hopefully the results of this may shed some light into picking better parameters for the mesh-based models, on which one currently relies for larger simulations.

3. Background

3.1 SPH model

SPH is a mesh-free Lagrangian method able to solve the general equations of fluid dynamics. Particles are used to discretize the field variables in the computational domain through a kernel approximation. (Rota, 2013) The motion of each particle is solved at each time step through a lagrangian approach, and field information (such as speed, pressure or density) is calculated for each particle. Each particle is a discrete element used to numerically integrate the partial differential equations expressing momentum and mass conservation.

3.2 Swash as a component of run up

An important concept of coastal hydrodynamics is run up (Stockdon, 2006), the height of discrete water-level maxima, which depends on two dynamically different processes: time averaged wave setup and total swash excursion. The former is parameterized by a dimensional form of an Iribarren-based expression, which mainly considers the foreshore beach slope, the offshore wave height, and the deep-water wavelength. The latter, Swash, is the focus of this paper, and its effects can generally be observed as the time-varying location of the intersection between the ocean and the beach. Two frequency bands parameterize the swash: the incident and infragravity bands. The incident is also parameterized by a dimensional form of an Iribarren- based expression. The infragravity is modeled dimensionally using offshore waveheight and wavelength, and shows no statistically significant linear dependence on foreshore or surf-zone slope. (Stockdon, 2006)

3.3 The energy conversion and interchange between incoming waves and swash

The energy spectra of runup can be dominated by low-frequency infragravity motion (0.004-0.05 Hz) below the seas swell frequency range (0.05-0.4 Hz) that normally dominates the offshore wave spectrum. The frequency downshift implies dissipation of waves at sea swell frequencies, as well as energy transfer to gently sloping infragravity waves (Guedes, 2013). This phenomenon is observed in the data collected at La Jolla (see fig 9), and one, which is hoped to be verified by the model when offshore waves are modeled with an irregular representative sea spectrum.

3.4 Spectral Decomposition of forcing waves of the SPH model

After running the model first with offshore monochromatic waves, the wave spectrum was broken up into the two modes described in 3.2, namely the incident and infragravity modes. Representative amplitudes were found for each region using Eq 7 below. Section 3.5 describes how the model piston parameters, stroke (S_{piston}) and frequency (f_{model}), were subsequently calculated.

3.5 Conversion of real wave parameters to scaled model piston stroke and frequency

To reduce computation space and time, the model's bathymetry and offshore wavelength were geometrically scaled by a factor of 10 and the frequency scaled using Froude number equivalence (Eqs 1-4 below). The representative wave amplitude for each wave mode was found from eqs 6-8. Finally the model piston stroke was found from eq 9 (Dean, 1991).

$[Eq.1]\ L_{model} = \frac{L_{real}}{10}$; model geometric scaling

$[Eq.2]\ h_{model} = \frac{h_{real}}{10}$

[Eq.3] $\lambda_{model} = \frac{1}{10} \times \frac{\sqrt{g h_{real}}}{f_{real}}$; shallow water dispersion relation where g= 9.81ms^{-2} and h_{real}=6m ;(depth offshore)

[Eq.4] $f_{model} = \sqrt{10} \times f_{real}$; model frequency

[Eq.5] $k_p = \frac{2\pi}{\lambda_{model}}$; wave number

[Eq.6] $m_0 = \int (energy\ density\ spectrum)\ df;\ first$ spectral $moment$

[Eq.7] $a_{real} = \sqrt{2 \times m_0}$; real wave amplitude

[Eq.8] $a_{model} = \frac{a_{real}}{10}$; model wave amplitude scaled geometrically

[Eq.9] $S_{piston} = a_{model} \frac{(\sinh 2k_p h_{model} + 2k_p h_{model})}{(\cosh 2k_p h_{model} - 1)}$; piston stroke

4. Methods & materials

4.1 Data collection

Field data collected near La Jolla, CA is used to evaluate the model simulations. Instruments were mounted on the 5 tripods shown in figure 3, as well as on 3 additional tripods in deeper water, extending out to 5 m water depth. This enabled observations extending from the swash, through the surf zone where waves are breaking, to deeper water outside of the surf.

Figure 3: Instrument setup: 8 tripods

Each one of these instruments is an acoustic Doppler velocimeter that measures the flow parallel to the prongs. The lowest sensor to the right shown in figure 4 is the one that is important for this paper, since it measured the flow going up and down the beach about 2 cm above the sand.

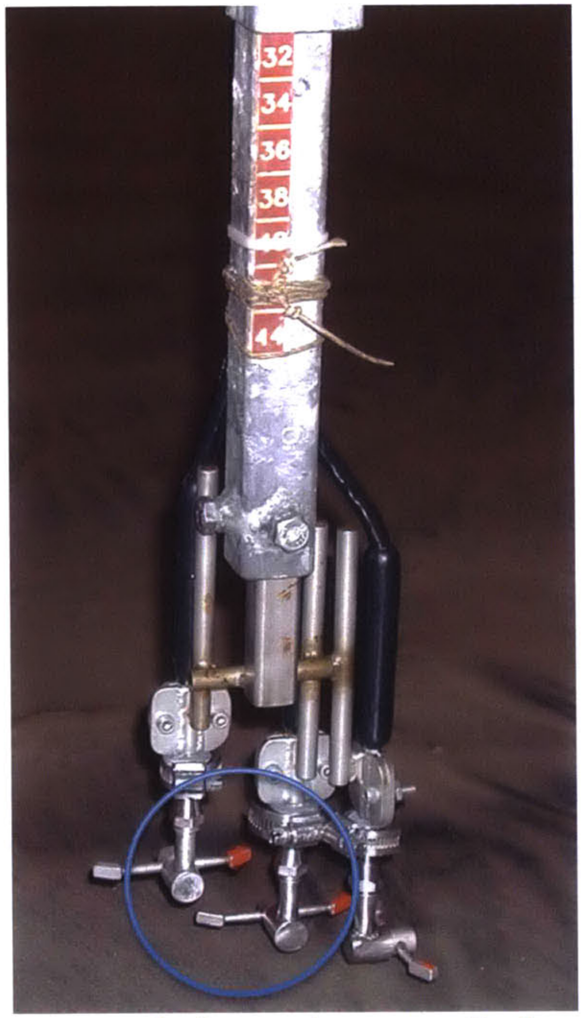

Figure 4: Close up on one instrument: an acoustic doppler velocimeter

4.2 Data Selection

With fortran and Matlab, raw data was sifted through to identify 1 hr long data runs where 4 conditions are met:

1. Incident waves ≈ normal to beach ($|\vartheta| < 2°$)
2. All sensors in swash zone versus surf zone (significant height<8cm)
3. Sensors are not buried, but are just above the sea bed (significant height>3cm)
4. The off shore forcing waves were of a variety of heights (significant heights were 0.5m, 0.68m, 1m)

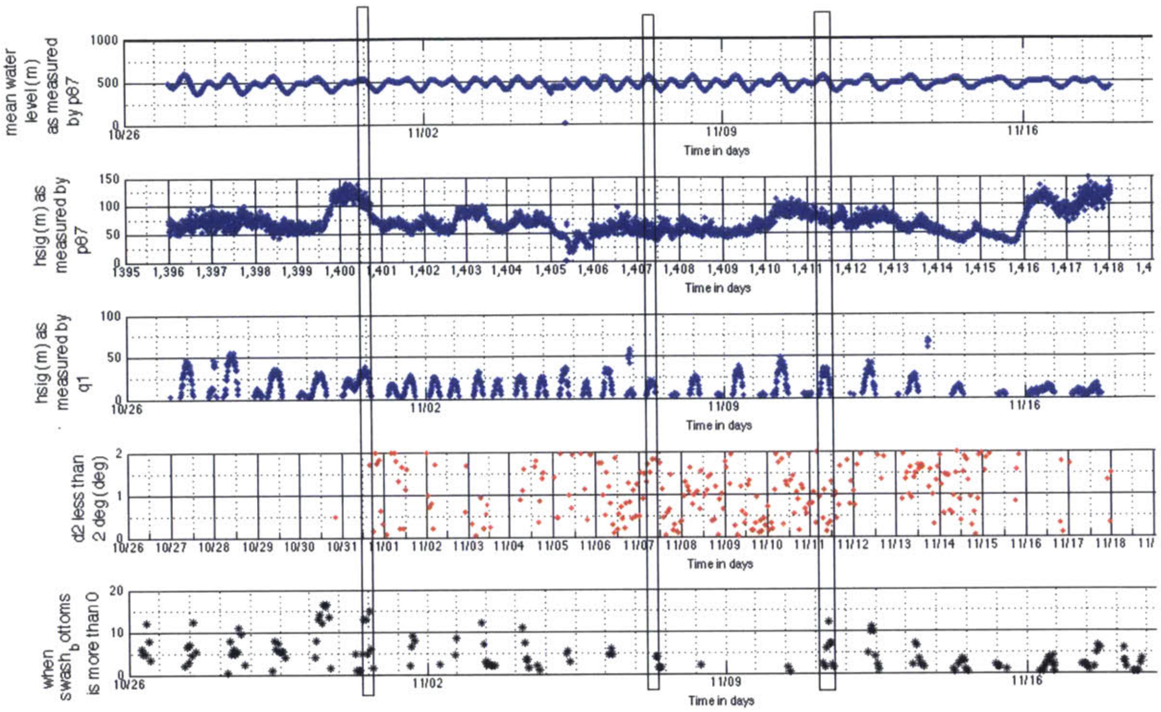

Figure 5: tool created to help select desirable runs for model verification

Figure 5 was one of the main figures initially used to search for desirable runs.
The third panel is the significant heights of cross shore swash sensors (with heights less than 3cm filtered out). The red dots in the 4th panel show the incident direction (near normal, only with magnitudes smaller than 2°). Black stars in the 5th panel show times when sensors are not buried in sand. Rectangles enclose intervals from which 1hr runs were chosen to verify the model.

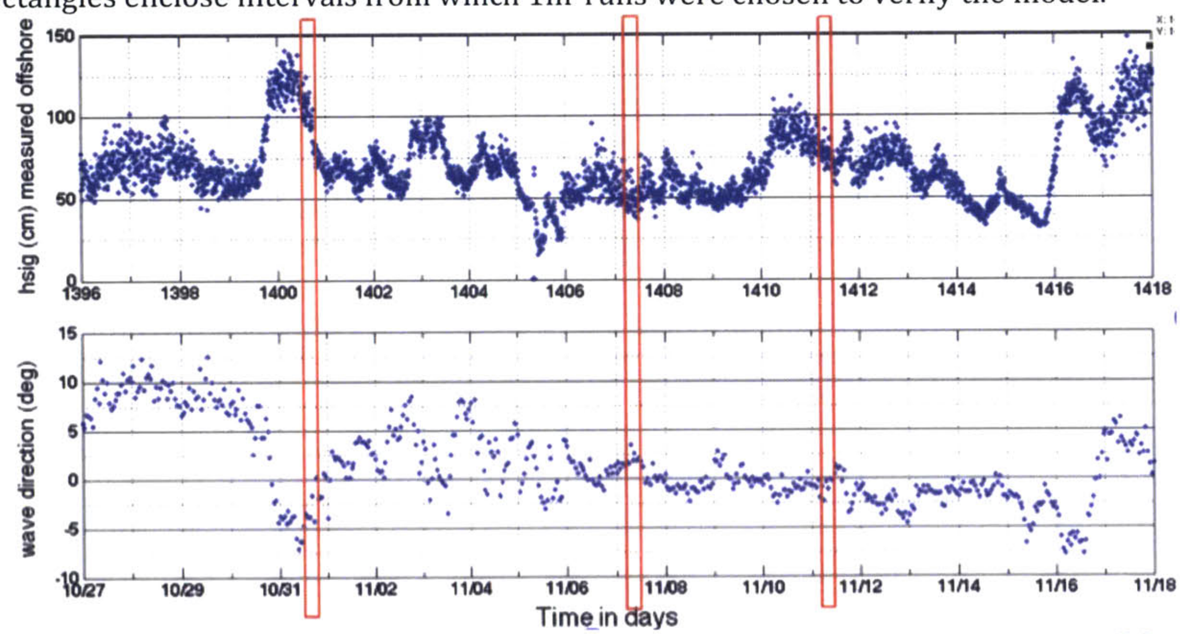

Figure 6: A graphical summary of the data over time where the first panel shows offshore significant wave height and the second shows incident wave direction.

Figure 6 was another data analysis tool, showing two quantities:

1. Offshore significant height

2. Incident wave direction

Enclosed in red rectangles, one can see the selected three desirable time intervals of a few hours from which 1 hr intervals are chosen. These three times also include a variety of forcing off shore wave heights: 100cm, 68cm, and 50cm.

4.3 Data Analysis

With the runs selected, conditions for future model/data comparisons had to be created. These included energy spectra for velocities and pressure, the cross shore setup profile, variance profile, velocity profile. To demonstrate this process, out of the 6 runs currently selected, the wave and flow behavior to be modeled will be examined for one of them: 31st Oct from 4pm-5pm.

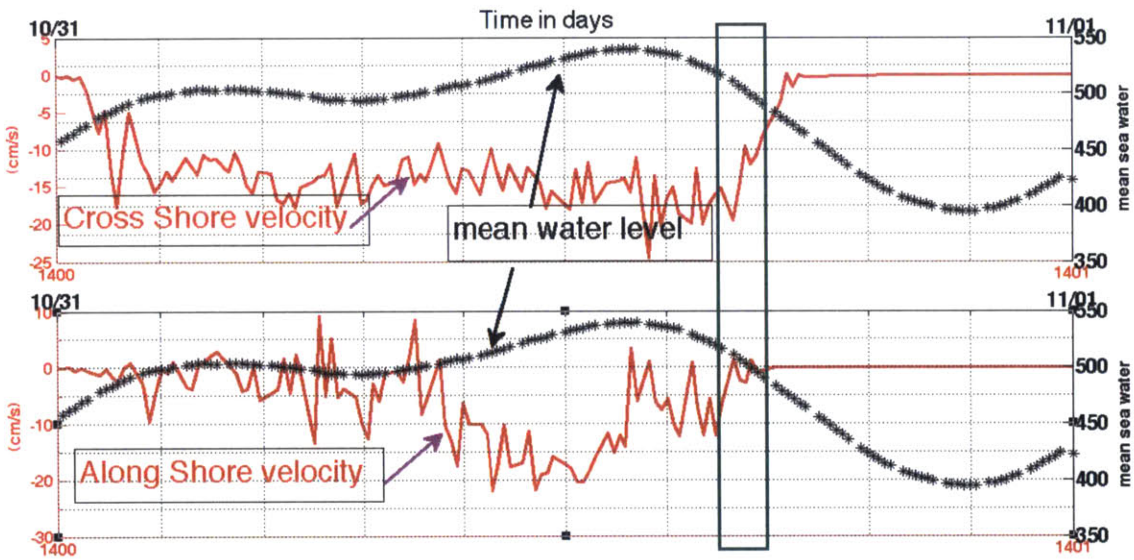

Figure 7: A close up on the mean cross shore and along shore velocities superimposed on the mean tide for the day containing the first desirable time interval (31st oct)

From figure 7, one may see that at low tide, the swash sensors are dry.

Also, cross-shore mean flows are negative due to the conservation of mass where the uprush is deeper than the backwash, and so mean backwash flow must be stronger to get all the water back offshore in the thinner tongue.

More over, the second panel verifies that at the time of the chosen run, the alongshore flows are negligible when compared with the cross shore flows. This therefore fits the situation in the model setup where the waves are normally incident.

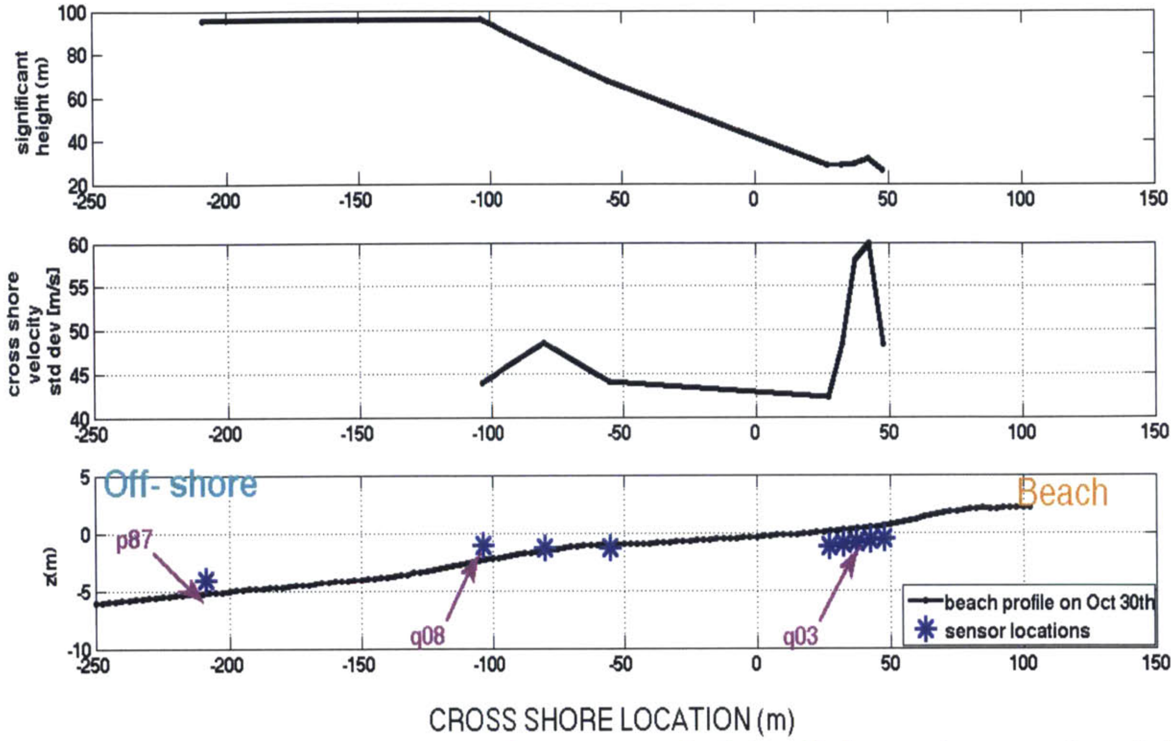

Figure 8: Variation of quantities in cross shore space. Left is off shore, then moving right will take you through the surf zone then finally onshore

Figure 8 displays the variation of quantities in cross shore space. The most off shore is to the left and moving right, one moves through the surf zone before reaching the beach. This is evident in the 3rd panel, which shows the beach profile. In that same panel, the blue stars are the locations of the sensors.

From the 1st panel which shows significant height versus cross shore location, one may see that wave heights decrease onshore owing to breaking wave dissipation.

From the 2nd panel which shows Cross shore variation of velocity standard deviation one may observe that the cross-shore velocity fluctuations remain relatively constant until reaching the swash, where velocity fluctuations must increase to conserve the energy flux.

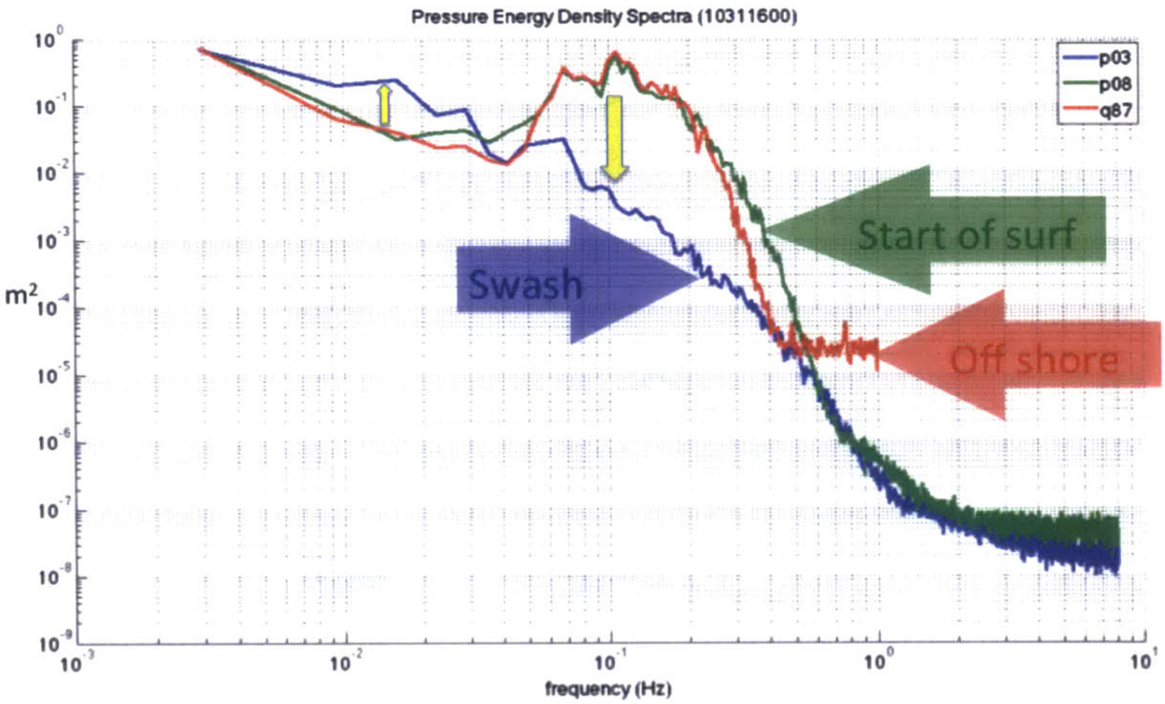

Figure 9: Pressure energy density spectra of the waves moving through 3 different cross- shore points

Figure 9 shows the pressure energy density spectra of the waves as they move through 3 different cross shore points. Comparing the three like this is a useful sanity check, as well as a means to understand what's happening during this hour. One may observe that the spectra of waves measured offshore is similar to those measured at the start of the surf zone, as one would hope, since not much energy has yet been dissipated. However, in the swash, the incident peak (at 0.1Hz so waves are coming in every 10 sec) has dropped due to dissipation, and the infragravity peak has increased since conservation of energy forces an increase in the infragravity peak, in order to carry the same amount of energy in the reduced water depth (Guedes, 2013). This mechanism describes how the tsunami approaches the coast looking unintimidating, only to shoal up at the beach. See figure 10. Infragravity waves are analogous to the tide, which does not dissipate energy as it comes in.

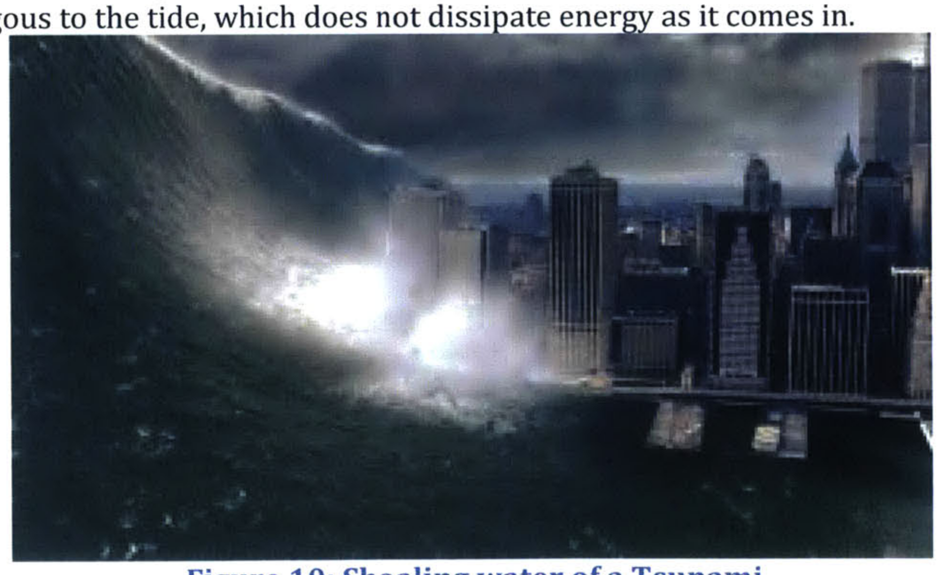

Figure 10: Shoaling water of a Tsunami

Now focusing on velocities in the swash, figure 11 shows more energy density spectra. but this time, of the cross and alongshore velocities in the swash. Here one may observe that the alongshore energy is much less significant than the cross shore, as is desired, since alongshore flow won't be considered in the model.

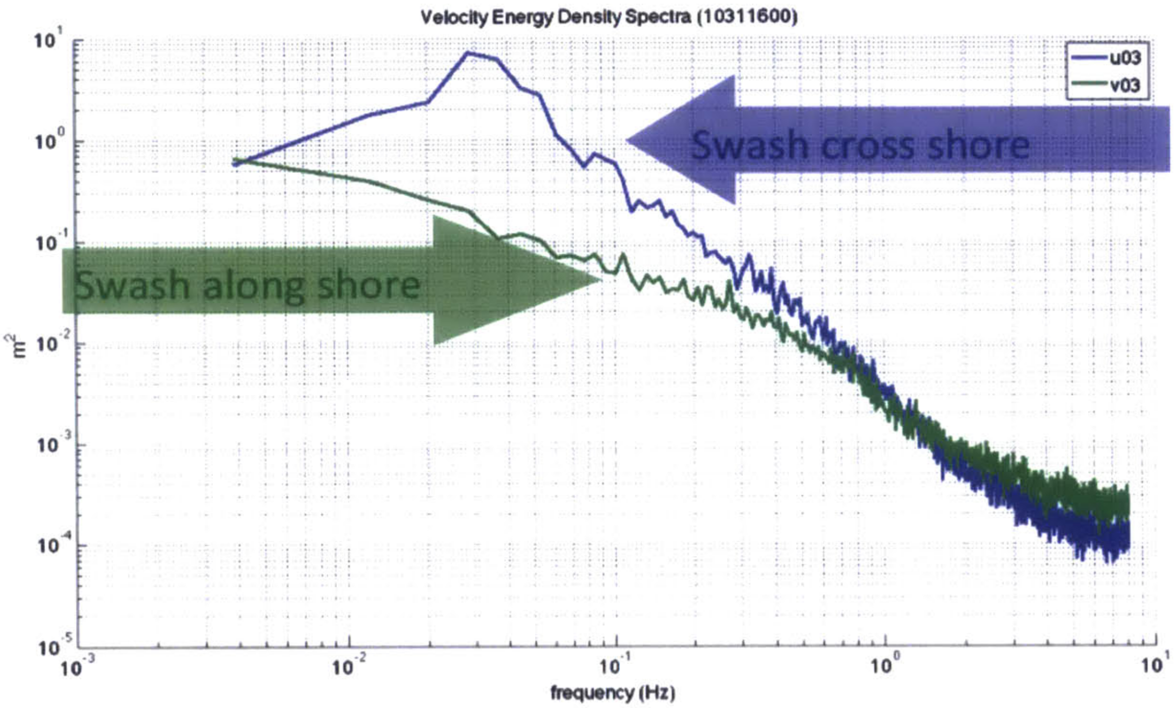

Figure 11: Velocity energy Density spectra in swash

Again, though now looking at the offshore characteristics, one can see that the energy in the alongshore velocity profile is again less than the cross shore, confirming the evaluation that waves are almost normally incident.

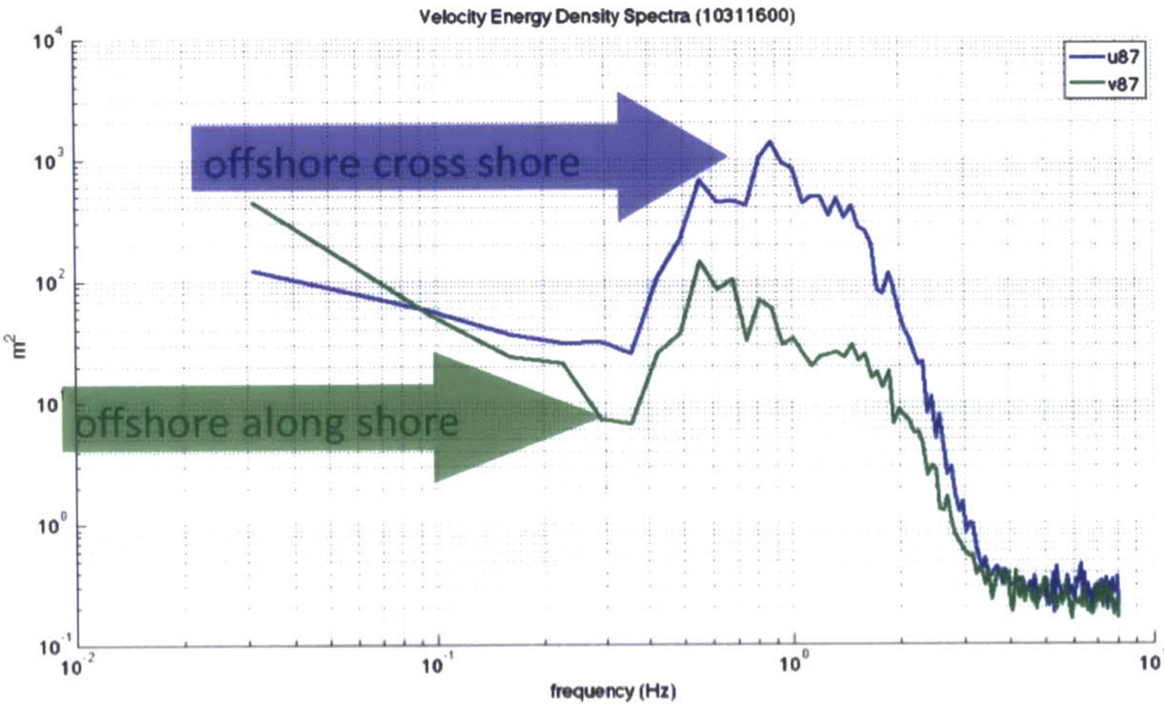

Figure 12: Velocity energy density spectra off shore

4.4 Model Runs

The SPH model was run and iteratively adjusted, inputting equations 1-9 to calculate parameters as described in section 3. The bathymetry was initialized with a geometric scale reduction of 10, and the system was forced by waves composed of a sum of two representative wave profiles. These were namely the infragravity and incident components of the wave spectrum.

5. Future plans

An outline of work to be completed is as follows:

- Evaluate model predictions in surf and swash
  - Compare Hsig and velocity fluctuations
  - evaluate cross-shore structure of waves and flows
  - evaluate changes with changing wave conditions
- Use the model to investigate the vertical swash structure and turbulence

6. Acknowledgements

None of this could have been possible without input from many people; in particular:

- The guidance of MIT professor Stefano Brizzolara
- The patient guidance of Britt Raubenheimer, Steve Elgar and group
- The support of WHOI
- The efforts of the PVLAB field crew to collect these data
- Funding by the Office of Naval Research for the field effort

7. Works Cited

Dean, R. (1991). *Water Wave Mechanics for Engineers and Scientist* (Vol. 2). FL: World Scientific Publishing Co.

Gorrell, L. (2011). SWAN predictions of waves observed in shallow water onshore of complex bathymetry. *Elsevier* , 510-516.

Guedes, R. (2013). Observations of wave energy fluxes and swash motions on a low-sloping, dissipative beach. *Journal of Geophysical Research* , *118*, 3651-3669.

Raubenheimer, B. (2002). Observations and predictions of fluid velocities in the surf and swash zones. *Journal of Geophysical Research* , *107*, C11.

Rota, R. A. (2013). *Numerical Modelig of Breaking Periodical Waves on a Sloped Beach Profile by SPH.* MIT sea Grant College Program. Cambridge: unpublished.

Stockdon, H. (2006). Empirical parameterization of setup, swash, and runup. *Elsevier* , 573-588.